

# Changes in the Oscillation Mode Shapes and Natural Oscillations of the Steel Beams Depending on the Beam Web Rigidity

V Volkova<sup>1</sup>, I Smolii<sup>1</sup>

*1. Department of Construction, Geotechnics and Geomechanics, SHEI "National Mining University", 19 Karl Marks Ave., Dnipropetrovsk 49000, Ukraine*

*E-mail: drvev@mail.ru, sebrle@bk.ru*

**Abstract:** The object of study is the steel span structures of conveyor galleries which is a widely used beam system span. Technological loads acting on the building construction conveyor galleries are dynamic in nature due to the force. This article presents the results of numerical simulation of dynamic behavior of welded metal beams in conveyor galleries. Investigations were carried out for the beams having symmetrical cross-sections and evenly-spaced transversal ribs with various spacing between the ribs in different beams. The regularities of changes in the oscillation mode shapes depending on the beam geometric characteristics have been investigated.

**Keywords:** dynamic; oscillation; beam; steel; conveyor galleries.

## 1. Introduction

Belt conveyors have gained widespread acceptance for charging materials along the belt-conveyor trestles into the blast furnaces in the metallurgical coal-preparation and ore-dressing plants, for transporting extracted materials onto the surface in the open pit and underground mining, in the building and construction sector as well as in other industries. Belt conveyors are installed in adequate buildings and premises or in purpose-built galleries between these structures [1].

The experience gained in the 70-year period of industrial operation of the galleries in Ukraine proves that these structures belong to the class of facilities of the first criticality level. High damage rates in the galleries stem from the concurrent effects of a number of adverse factors, including dynamic loads [2]. Compared to trusses, steel beams have higher reliability and lower operational costs.

Articulated and thin-walled beams, parallel-chord trusses, rectangular and circular cylindrical shells as well as other types of structural elements can be used as span bearing structures. From the point of view of cost saving and operating economy, the application of beam bearing structures is rational for the spans up to 30 m in length, while for the spans ranging from 24 m to 42 m it is recommended to use lattice girders as the load-bearing structures, particularly trusses. Shells may also be used as the load-bearing structures in the conveyor galleries with the spans exceeding 30 m in length [2]. They have higher reliability and require less operating expenditures as compared to trusses. Depending on technological requirements, the span structures of conveyor galleries can be installed straight or inclined (10-15°) [6]. Technological loads acting upon the structural elements of conveyor galleries are of dynamic nature. Due to this fact, investigations into dynamic characteristics of the span structures of conveyor galleries are the matter of topical interest.

## 2. The object of research

The objects of this research are conveyor gallery span structures. These structures are the facilities of the first criticality level. With an aim to ensure the best reliability, strength and stability of span structures at all stages of their manufacturing, transportation and erection, the up-to-date Regulations and Standards of construction practices provide guidance to the selection of geometrical parameters and stiffness characteristics for the span structures.

In the real-world beam structural systems, a number of initial imperfections of the elements can be found, in particular, bent portions, curvature bending under transverse loads, and other defects. For this reason, the limit ratio of  $b_f/t_f$  as recommended in the Standards is slightly less than the value obtained on the basis of an idealized design scheme [3].

According to the State Standards and Norms for construction in Ukraine (DBN V.2.6-163: 2010), the conventional boundary slenderness parameters should be set as  $\bar{\lambda}_{uf} = 0,36 + 0,1\bar{\lambda}$ , for the beam chords and  $\bar{\lambda}_{uw} = 1,30 + 0,15\bar{\lambda}^2$  for the web. In this case, the parameter  $\bar{\lambda}$  is conventional slenderness of the structural

framing, which is determined by taking into account the overall stability of the system under the action of the central compression force [4].

Technological loads acting on the structural elements of conveyor galleries are dynamic in nature, due to induced oscillations of the conveyor belt transporting bulk material at various stages of operation. Due to this fact, investigations into dynamic characteristics of the span structures of conveyor galleries are of great significance.

Formerly, when calculating conveyor gallery structures, the most commonly used method was based on the flat cross-section hypothesis [10]. However, for dynamic behavior of beams in the span structures, such approach is rather approximate. The models suggested by Timoshenko and Vlasov have also found a wide application [7]. Practical convergence of the research results is ensured by the repeatability of the values obtained when changing a finite element mesh [5].

### 3. The method of investigations

Simulation was performed for simply supported pin-ended beams. The results were obtained with the use of the SCAD software package and implementation of Lanczos method for dynamic analysis [8]. Rectangular finite element mesh was used in research. The finite elements represented the plates of 100×100 mm in size and 20 – 40 mm thick [11]. According to the standards, it is recommended to analyze from 3 to 5 principal modes of oscillation. In order to avoid the building-up of errors in integration, simulation was carried out for 10 modes of oscillation. In further investigations the first 5 modes were used. The results obtained were compared to available approximate solutions [9].

The computation was performed using the finite element method with the SCAD PC Programming Software. The numerical analysis was performed in the computation of the beams with the specified geometrical characteristics. The reduced values of slenderness of the beam webs varied within the range of  $\bar{\lambda}_w = 2.5 \div 13$  and the slenderness ratios of the beam chords varied within the particular range of  $b_f/t_f = 10 \div 40$ .

The boundary conditions corresponded to a hinged structure. Dimensions of the beam cross sections were chosen in accordance with the recommendations in “The Handbook on Conveyor Gallery Designs”, the Supplement to SNiP (Local Building Requirements) 2.09.03-85”. The data were obtained for the I-section welded beam of the span length of 12 m. The web of beam was connected with the flanges via filled welds. Disposition, effective throat thickness and effective length of welds were chosen in accordance with the recommendations.

The finite elements used in the simulations represented “four-node rectangular plates” (FE-analysis 13), i.e. the plate members subjected to bending and lying in the plane XOY. The finite elements of this kind are generally useful in case of uniform thickness materials. In each node of these finite elements, three degrees of freedom were defined, namely:  $w$  - vertical displacement (sagging) and also  $UX$  and  $UY$  – the angles of rotation about the axes  $X$  and  $Y$ , respectively. The control points were chosen at equal intervals along the top and bottom flanges of the beam, as well as on the web. Displacements were controlled in the nodes of the finite elements.

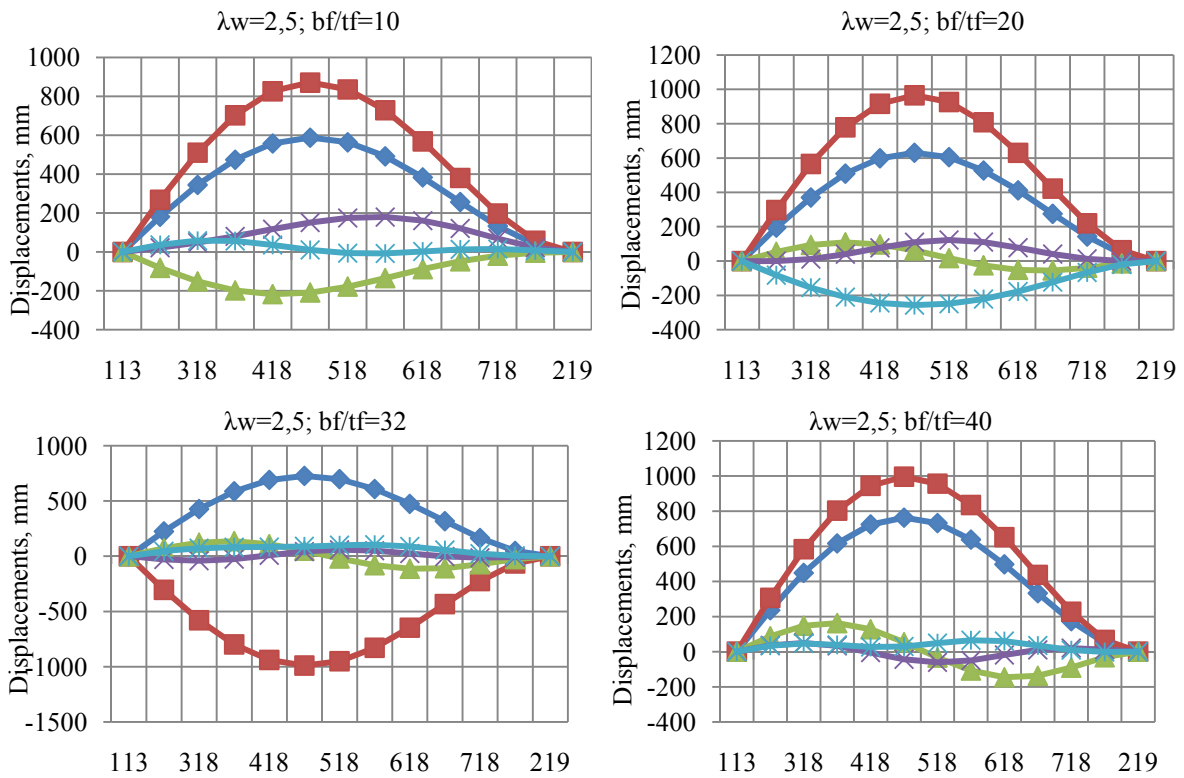
In the theory of the finite element method, a lot of attention is paid to the problem of convergence, i.e. the asymptotic behavior of the accuracy estimates of the obtained approximate solution with the unlimited thickening of the finite element mesh. Proceeding from the results of the assessment of convergence of both the compatible finite elements and the incompatible ones, convergence of the given finite elements can be estimated. The spacing's and density of the finite element mesh were chosen in accordance with the required accuracy of the approximate solution and also taking into account an uncertain error in the determination of stresses and deformations. According to the estimates given in the paper [5], the rates of convergence of the computing procedures for FE No. 13 came to 2 parameters for displacements, 2 parameters for moments and 1 parameter for transverse forces.

### 4. Analysis of the results obtained

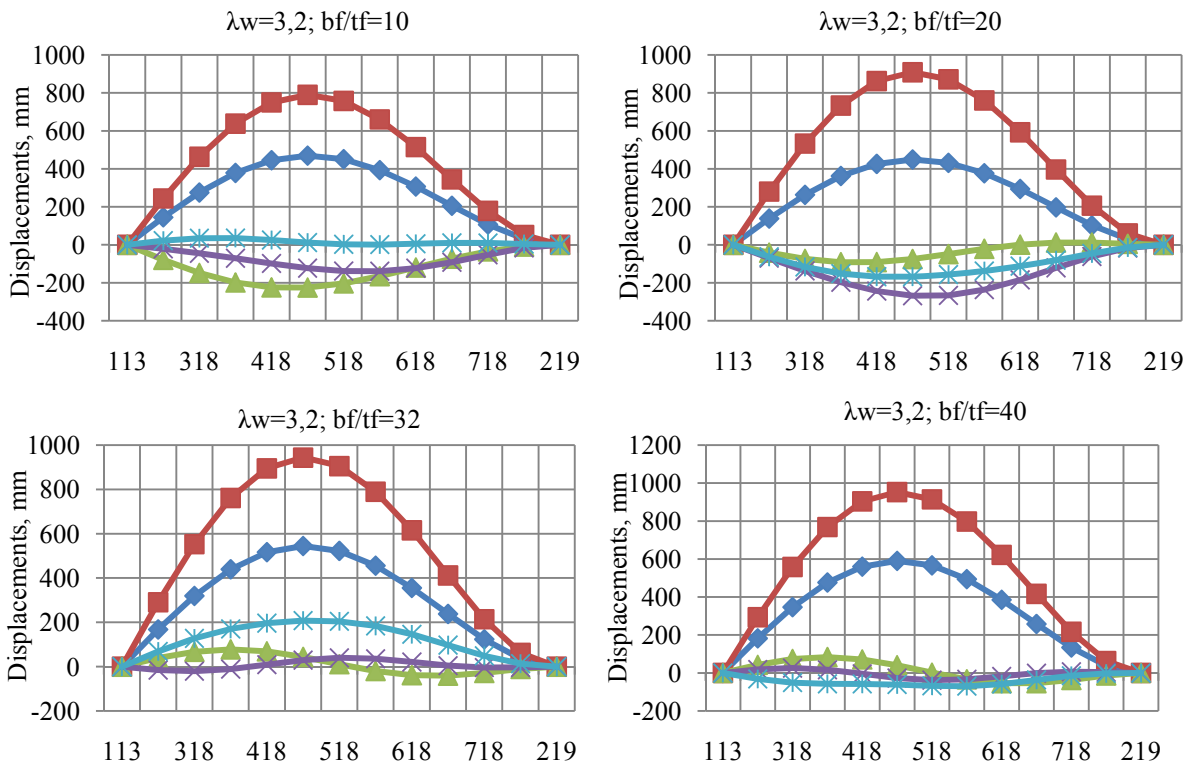
Based on the results of the calculation, the following regularities of changes in the oscillation mode shapes were determined for various reduced flexural capacities of the beam web and beam chord. In the tested slenderness range of the web  $\bar{\lambda}_w = 2.5 \div 5.5$  and that of the beam flanges  $b_f/t_f = 10 \div 40$ , the beams with the slenderness values of  $\bar{\lambda}_w = 2.5$  and  $\bar{\lambda}_w = 3.2$  belong to the beams with the rigid web and those with the slenderness value of  $\bar{\lambda}_w = 5.5$  are the beams with the flexible web. The mode shapes for flanges are given in Figure 3 ( $\bar{\lambda}_w = 2.5$ ), Figure 4 ( $\bar{\lambda}_w = 3.2$ ), Figure 5 ( $\bar{\lambda}_w = 5.5$ ).

The first type of the oscillation mode shapes in the beam flanges corresponded exclusively to node free mode shapes. The oscillation phase was constant. A single shift of the oscillation phase was revealed in the transition of the ratio  $b_f/t_f$  from value 10 to value 20. The effects of the slenderness characteristics of the beam flanges and webs upon the oscillation mode shapes of the second type are of the following nature. The beams demonstrated a

node free mode shapes of oscillations. The shifts of the oscillation phases were observed with the value of  $\bar{\lambda}_w = 2.5$  in the transition of the ratio  $b_f/t_f$  from value 20 to value 32 and from value 32 to value 40.



Mode Shape 1 — Mode Shape 2 — Mode Shape 3 — Mode Shape 4 — Mode Shape 5  
**Figure 1 Oscillation mode shapes in the beam flanges  $\bar{\lambda}_w = 2.5$ .**



Mode Shape 1 — Mode Shape 2 — Mode Shape 3 — Mode Shape 4 — Mode Shape 5  
**Figure 2 Oscillation mode shapes in the beam flanges  $\bar{\lambda}_w = 3.2$ .**

The shifts of oscillation phase were detected with the value  $\bar{\lambda}_w = 5.5$  in the transition of the ratio  $b_f/t_f$  from value 10 to value 20. When the ratio  $b_f/t_f$  changed from value 20 to value 32, the transition from the node free oscillation mode shapes to the single-node modes occurred.

The oscillation mode shapes of the third type changed from the node free oscillation mode shapes to the single-node ones in the transition of the ratio  $b_f/t_f$  from value 10 to value 20. In the transition of the ratio values of  $b_f/t_f$  from 20 to 32 with the parameter  $\bar{\lambda}_w = 5.5$ , the node free oscillation mode shapes transformed into the two-node modes.

In the fourth type of oscillation mode shapes, with the web slenderness reduced value  $\bar{\lambda}_w = 2.5$ , the transition of the oscillations from the node free modes into the single-node modes was observed when the ratio values of  $b_f/t_f$  changed from 10 to 20, but when the ratio values of  $b_f/t_f$  changed from 20 to 32, the single-node modes transformed into the two-node mode shapes. At the same time, the transition from the node free mode shapes to the two-node modes took place when the ratio values  $b_f/t_f$  changed from 20 to 32 and the value  $\bar{\lambda}_w = 3.2$ . The node free mode shapes are characteristic only for the value  $\bar{\lambda}_w = 5.5$ . Phase shifts were observed in both cases of transition of the ratio  $b_f/t_f$  from value 10 to value 20 and from value 20 to value 32.

The following changes are peculiar to the fifth type of the oscillation mode shapes. With  $\bar{\lambda}_w = 2.5$ , the two-node mode shapes are typical for the value  $b_f/t_f=10$ , while the node free modes are characteristic of the ratios  $b_f/t_f = 20$  and  $b_f/t_f = 32$ . Only the node free oscillation modes were revealed with  $\bar{\lambda}_w = 3.2$  and  $\bar{\lambda}_w = 5.5$ , at that, with the value  $\bar{\lambda}_w = 5.5$ , phase shifts took place in the whole range of changes of the ratio values  $b_f/t_f = 10 \div 40$ .

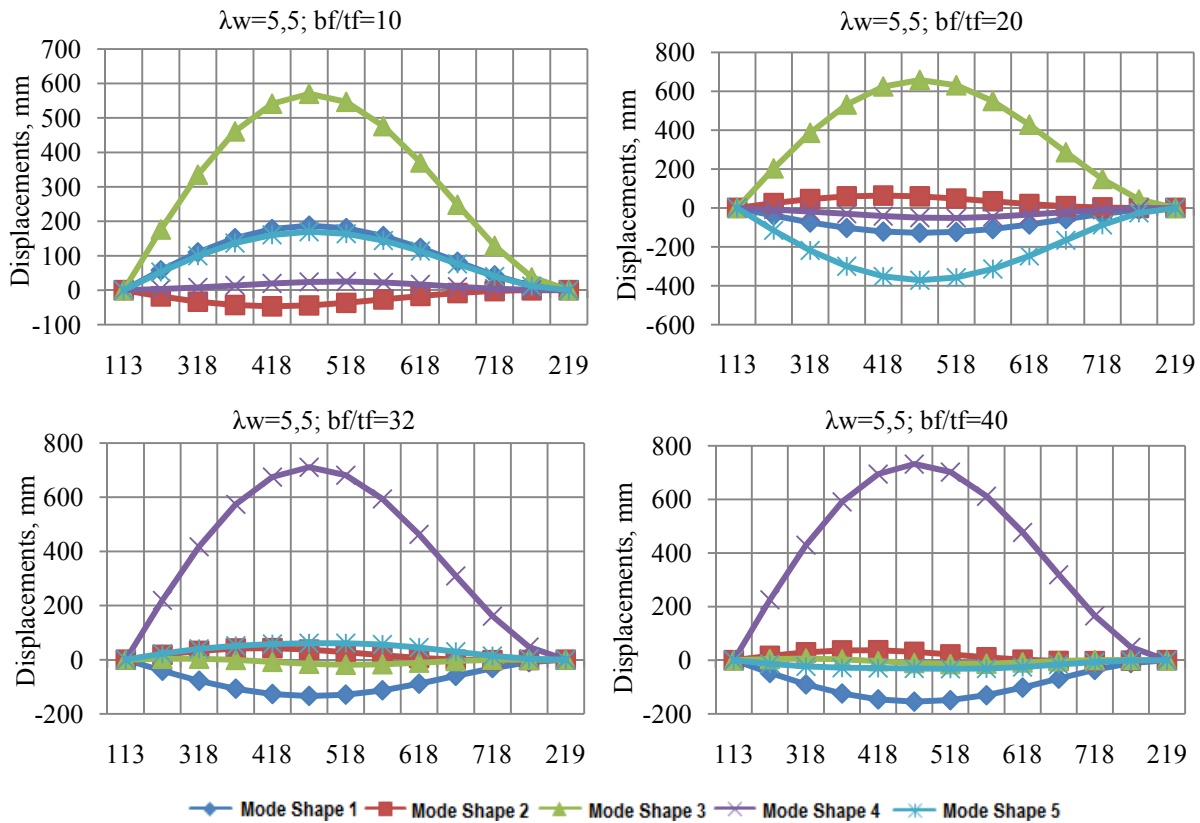
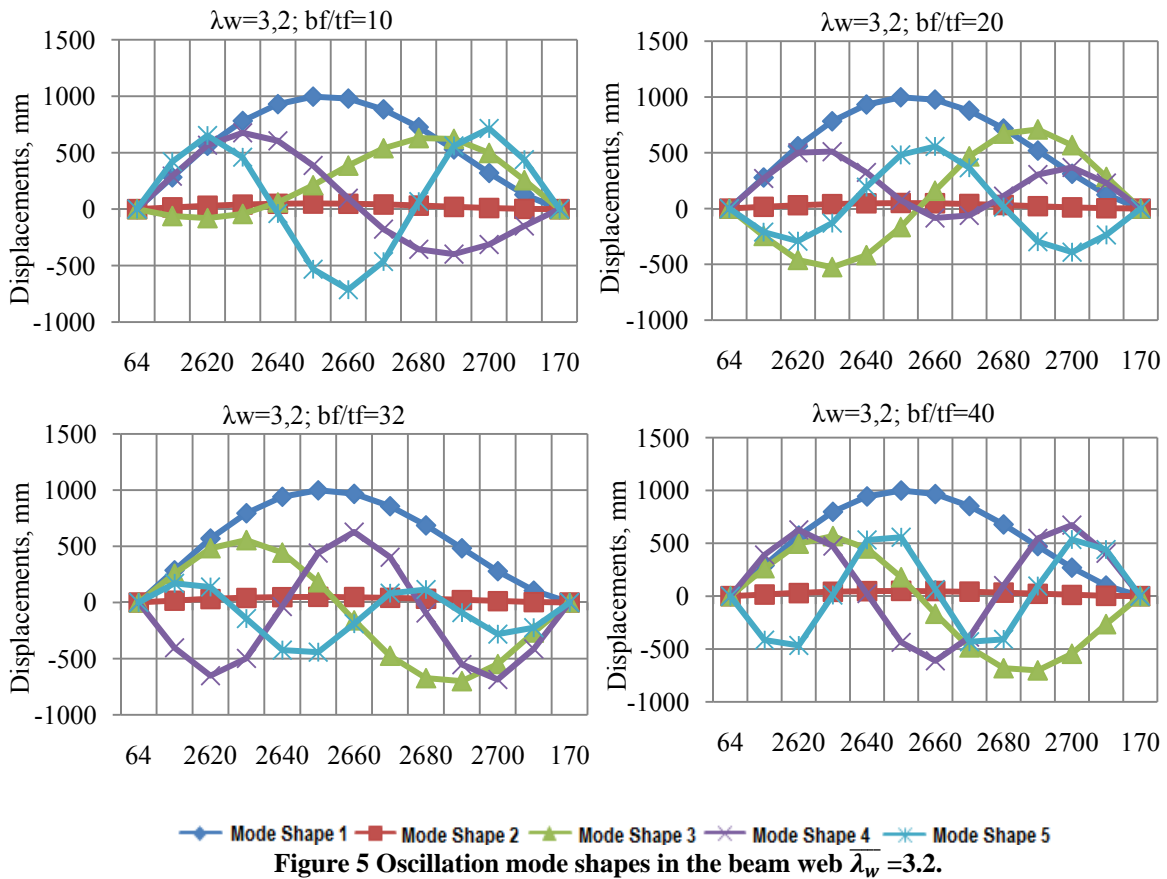
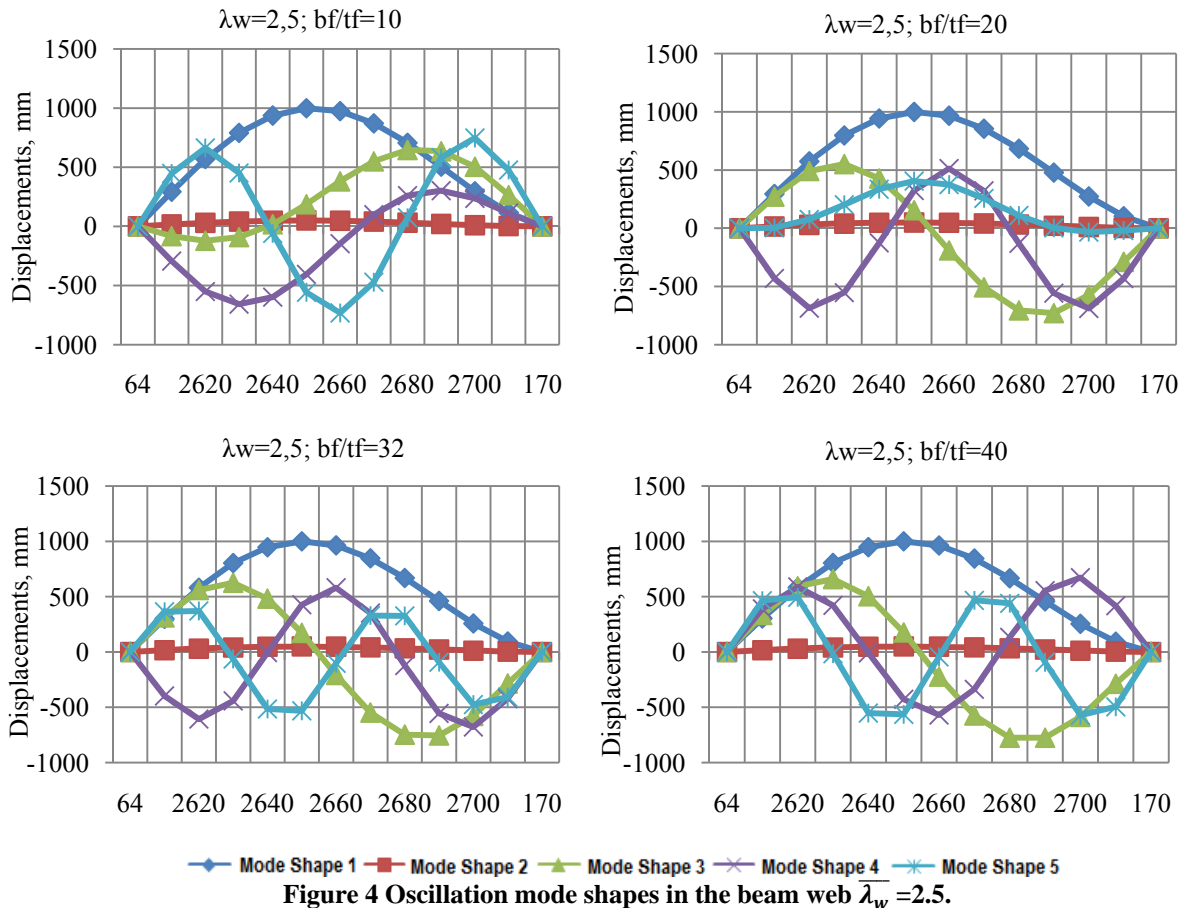


Figure 3 Oscillation mode shapes in the beam flanges  $\bar{\lambda}_w = 5.5$ .

The following regularities were revealed in the oscillations of the beam web. The mode shapes for the web are given in Figure 6 ( $\bar{\lambda}_w = 2.5$ ), Figure 7 ( $\bar{\lambda}_w = 3.2$ ) and Figure 8 ( $\bar{\lambda}_w = 5.5$ ). The node free mode shapes corresponded to the first type of oscillations. With the value  $\bar{\lambda}_w = 5.5$ , phase shifts in oscillations occurred in the transition of the ratio  $b_f/t_f$  from value 10 to value 20.

At the same time, the node free mode shapes represented the second type of oscillation modes. The single-node mode shapes are characteristic of the value  $\bar{\lambda}_w = 5.5$ , and phase shifts were detected when the ratios of  $b_f/t_f$  changed from value 10 to value 20.

The single-node mode shapes were characteristic of the third type of oscillations. Phase shifts were revealed with the value  $\bar{\lambda}_w=2.5$  in the transition of the ratio  $b_f/t_f$  from value 10 to value 20, and with the values of  $\bar{\lambda}_w= 3.2$  and  $\bar{\lambda}_w= 6$ , phase shifts took place in the transition of the ratio  $b_f/t_f$  from value 20 to value 32.



With the value  $\bar{\lambda}_w = 5.5$ , the transition from the node free mode shapes to the two-node oscillation modes occurred when the ratio  $b_f/t_f$  changed from value 20 to value 32.

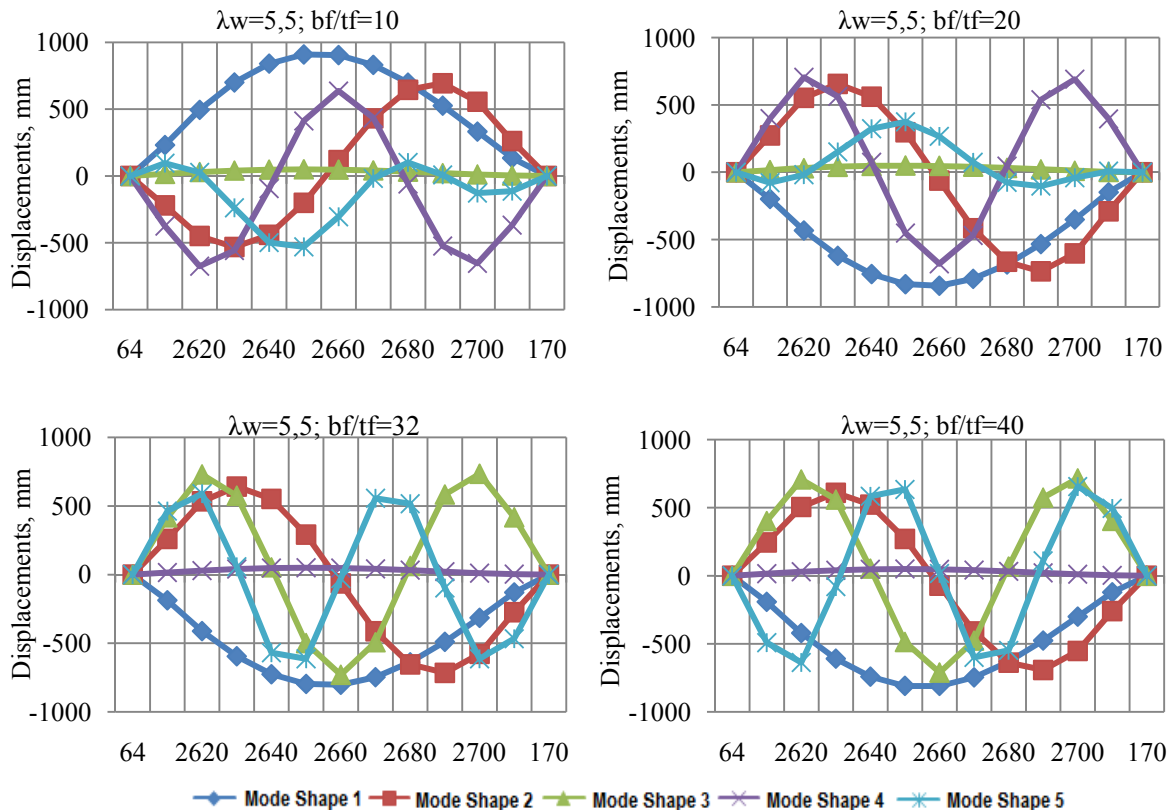


Figure 6 Oscillation mode shapes in the beam web  $\bar{\lambda}_w = 5.5$ .

The transition of the oscillations from the single-node modes into the two-node modes was observed when the ratio  $b_f/t_f$  changed from value 10 to value 20. With the same values of  $\bar{\lambda}_w$ , phase shifts were revealed when the ratio  $b_f/t_f$  changed from value 32 to value 40. With the value  $\bar{\lambda}_w = 5.5$ , the two-node oscillation modes transformed into the node free modes in the transition of the ratio  $b_f/t_f$  from value 20 to value 32, and phase shifts were detected when the ratio  $b_f/t_f$  changed from value 10 to value 20.

Table 1 Natural frequencies in the beam  $\bar{\lambda}_w = 2.5$

$\bar{\lambda}_w$	2,5			
$b_f/t_f$	10	20	32	40
1	11,39288	9,366584	8,14479	7,582385
2	14,83799	13,38536	12,23208	11,66954
3	21,51133	17,16554	16,14953	15,6817
4	23,98901	21,83745	20,25719	19,81077
5	29,3693	23,00132	24,4384	23,90104

The changes of the  $\bar{\lambda}_w$  and  $b_f/t_f$  parameters have more complex effects on the fifth type of the beam web mode shapes. With the value of  $\bar{\lambda}_w = 2.5$ , during the transition of the ratio  $b_f/t_f$  from value 10 to value 20 and when the ratio  $b_f/t_f$  changes from value 20 to value 32, the single-node mode shapes passed into the two-node oscillation modes; and when the values of the ratio  $b_f/t_f$  ran from 32 to 40, phase shifts were detected. At the same time, with the value of  $\bar{\lambda}_w = 3.2$ , the two-node oscillation mode shapes evolve into the three-node modes when the ratio  $b_f/t_f$  was passing from value 20 to value 32, while the oscillation phase shifts were observed in both cases – when the ratio values of  $b_f/t_f$  were going from 10 to 20 and from 32 to 40. With the value of  $\bar{\lambda}_w = 5.5$ , the three-node modes with the phase shifts were revealed in the whole range of the varying parameter  $b_f/t_f = 10 \div 40$ .

**Table 2 Natural frequencies in the beam  $\bar{\lambda}_w = 3.2$**

$\bar{\lambda}_w$	3,2			
$b_f/t_f$	10	20	32	40
1	11,55461	9,285806	8,249276	7,766684
2	14,96826	13,73886	12,68756	12,14963
3	19,53935	14,95608	13,51907	13,14629
4	21,90456	18,92241	16,66132	16,06623
5	25,66004	19,38699	19,93151	19,31296

**Table 3 Natural frequencies in the beam  $\bar{\lambda}_w = 5.5$**

$\bar{\lambda}_w$	5,5			
$b_f/t_f$	10	20	32	40
1	11,23811	8,005485	6,856546	6,570212
2	15,04187	11,90746	9,377694	8,675607
3	15,14355	14,34913	11,8757	10,79307
4	16,47144	14,73602	13,57126	13,13114
5	17,46575	15,82215	14,36111	13,32122

The changes in natural frequencies are shown in Tables 1, 2 and 3 for the values of 1, 2 and 3, for the values  $\bar{\lambda}_w = 2.5, 3.2$  and  $5.5$  respectively. The curves representing the changes in the natural frequencies are shown in Figures 7, 8 and 9 correspondingly.

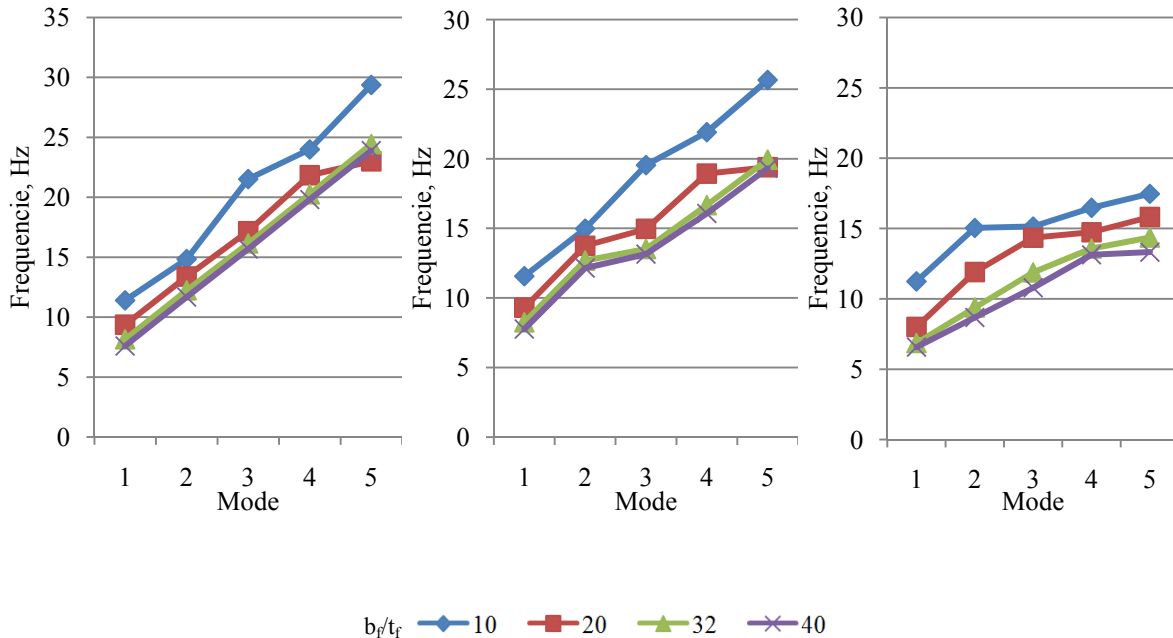


**Figure 7 Natural frequency for  $\bar{\lambda}_w = 2.5$**

**Figure 8 Natural frequency for  $\bar{\lambda}_w = 3.2$**

**Figure 9 Natural frequency for  $\bar{\lambda}_w = 5.5$**

From the results of investigations, we can come to the conclusion that the higher flexibility of the beam wall the lower the natural vibration frequencies, and this, in its turn, has a beneficial effect on the operational characteristics capabilities of the beam.

## 5. Conclusions

Based on the results of the calculation, the following regularities of changes in the oscillation mode shapes were determined for various reduced flexural capacities of the beam web and beam chord. In the tested slenderness range of the web  $\bar{\lambda}_w = 2.5 \div 5.5$  and that of the beam flanges  $b_f/t_f = 10 \div 40$ , the beams with the slenderness values of  $\bar{\lambda}_w = 2.5$  and  $\bar{\lambda}_w = 3.2$  belong to the beams with the rigid web and those with the slenderness value of  $\bar{\lambda}_w = 5.5$  are the beams with the flexible web. The mode shapes for flanges are given in Figure 3 ( $\bar{\lambda}_w = 2.5$ ), Figure 4 ( $\bar{\lambda}_w = 3.2$ ) and Figure 5 ( $\bar{\lambda}_w = 5.5$ ).

The first type of the oscillation mode shapes in the beam flanges corresponded exclusively to node free mode shapes. The oscillation phase was constant. A single shift of the oscillation phase was revealed in the transition of the ratio  $b_f/t_f$  from value 10 to value 20. The effects of the slenderness.

## 6. References

- [1] Gordeyev V N, Lantukh-Lyashenko A I, Pashinsky V A, Perel'muter A V, Pichugin S F 2007 Loads and effects on buildings and structures (Moscow: Publishing House of Association of Building Universities)
- [2] Gorev V V 2002 Metal structures. Volume 3, Special designs and constructions (Moscow: High School Publishing House)
- [3] Gorev V V 2002 Metal structures. Volume 1 Structural elements (Moscow: High School Publishing House)
- [4] The State Standards and Norms for construction in Ukraine (DBN V.2.6-163: 2010), Steel structures (Kiev: Minregionbud Publishing House of the Ministry of Regional Development, Construction and Housing and Communal Services of Ukraine)
- [5] Karpilovsky V S, Kriksunov E Z 2003 CAD System for users (Kyiv)
- [6] SNiP 2.09.03-85, Construction rules and regulations for industrial enterprises (The USSR State Committee for Construction)
- [7] Soltani M, Asgarian B, Mohri F 2014 Finite element method for stability and free oscillation analyses of non-prismatic thin-walled beams” (Thin Walled Structures vol. 82) pp 245-261
- [8] Fialko S 2007 The Lanczos method of displacements as applied for the seismic analysis of structures (CADmaster Magazine, vol 5) pp 102-105
- [9] Perel'muter A 2014 Discourse on Construction Mechanics Scientific Edition (Moscow: SCAD Soft).
- [10] Perel'muter A, Slivker V 2002 Computational Models of Structures and Feasibility of their Analysis Scientific Edition (Kiev: Stal Publishing House)
- [11] Zinkevich O K 1975 The finite element method in engineering (Moscow: Mir Publishing House)